Length Dependent Conduction of Polyynes: Searching for the Limit of the Tunneling Regime

Yueze Gao,*[a] Edmund Leary,[b] Lucía Palomino-Ruiz,[b, c] M. Teresa González,*[b] Maximilian Krempe,[d] Matthew Johnson,[a] and Rik R. Tykwinski*[a]

[a]Department of Chemistry, University of Alberta, 11227 Saskatchewan Drive, Edmonton, Alberta, Canada T6G 2G2. Correspondence to: rik.tykwinski@ualberta.ca

[b]Fundación IMDEA Nanociencia, Calle Faraday 9, Campus Universitario de Cantoblanco, 28049 Madrid, Spain. Correspondence to: teresa.gonzalez@imdea.org

[c]Departamento de Química Orgánica, Facultad de Ciencias, Unidad de Excelencia de Química Aplicada a Biomedicina y Medioambiente (UEQ), Universidad de Granada, 18071 Granada (Spain)

[d]Department of Chemistry and Pharmacy & Interdisciplinary Center for Molecular Materials (ICMM), Friedrich-Alexander-Universität (FAU) Erlangen-Nürnberg, Nikolaus-Fiebiger-Straße 10, 91052 Erlangen (Germany)

Abstract: Rigid, conjugated molecules are excellent candidates as molecular wires since they can achieve full extension between electrodes while maintaining conjugation. Molecular design plays a significant role, through minimizing the accessible pi surface to minimize interactions between the bridging wire and the electrode. Polyynes are archetypal molecular wires that feature both a rigid and a thin molecular framework with a cross-section of a single carbon atom. Understanding the behavior of polyynes in molecular junctions is essential for testing models of length versus electron transport. We report construction of molecular junctions using polyynes with a well-defined length up to ca. 5 nm in devices characterized by scanning tunneling microscopy break junctions (STM-BJ). The polyynes, **Py**[*n*]** (*n* = 4, 6, 8, 10, 12, 16), are endcapped with pyridyl groups, and we demonstrate good agreement between the length of the molecular junction and the calculated molecular length, with an average discrepancy of just 0.1 nm. This highlights the power of STM-BJ experiments to accurately determine molecular length. The range of molecular lengths studied, from 1.8 to 4.8 Å, mark this as the most accurate determination of β in polyynes to date (β = 2.2 nm^{-1}). We have applied a model based solely on the single and triple bond lengths to interpret these β-values, which predicts β = 1.9 nm^{-1}, consistent with the experimental value. This model also confirms that electronic coupling in polyynes is unaffected by the rotation about the single bonds. At all molecular lengths, we observe conductance in tunneling regime continues due to the long effective conjugation length of polyynes.

Keywords: conductance, molecular electronics, electron transport, polyyne, scanning tunneling microscopy break junctions.

The relationship between charge transport and molecular length is a fundamental aspect of molecular electronics, which typically involves using structurally well-defined molecules as building blocks in a bottom-up strategy.[1,2] Charge transport through a single molecule can be effectively measured using various techniques such as scanning tunneling microscopy break junctions (STM-BJ), mechanically controlled break junctions (MCBJ), and electromigration break junctions.[3] When measuring the conductance (G) of a series of oligomers as a function of molecular length (L) within a tunneling transport regime, the data typically follow an exponential relationship of the form:

$$G = G_c \exp(-\beta L) \qquad \text{(eq 1)}$$

where G_c, β, and L are the contact conductance, attenuation factor, and molecular length, respectively. The attenuation factor β is generally a characteristic property of the homologous series of oligomers under consideration. For example, alkane-bridged molecular junctions typically exhibit value of ca. β = 8–10 nm^{-1}.[4,5] When the saturated sp^3-carbon backbone of alkanes is formally replaced with a sequence of sp^2-carbons yielding an alkene structure, the attenuation factor decreases dramatically to β = 2.2 nm^{-1} as a result of conjugation.[6,7] Completing the transformation based on the hybridization to include sp-carbon, gives polyynes, for which a rather large range of values have been reported β = 0.6–3.2 nm^{-1}.[8][9,10] It is also noted that, in special cases, β can be close to zero or even negative, meaning that the conductance changes little or even increases with increasing length. Such behavior has been reported in sp-hybridized cumulenes[11,12] as well as cyanine dyes[13,14] and porphyrin tapes at elevated bias voltages.[15]

Accurate measurement of the size of molecular wires is essential for designing molecular devices, especially when the goal is to precisely place molecules into nanofabricated junctions. Molecular length can be established in the solid state by X-ray crystallography and in vacuo through molecular modelling. In solution, molecular modelling can predict the distribution of conformers for a molecule, which can be compared with experimental methods including EPR[16] and NMR spectroscopies,[17,18] X-ray scattering interference ruler,[19] and Förster resonance energy transfer (FRET) modelling.[20] At a single-molecule level, the STM-BJ technique has been shown to be capable of revealing differences in molecular length between *trans* (ca. 1.4 nm) and

cis (ca. 0.8 nm) cumulene isomers,[21] distinguishing between the closed and open forms of a molecular nanohoop,[22] as well as detecting mechanochemical atropisomerization.[23]

Experimentally establishing the relationship between the molecular length and gap size of an electrode by the STM-BJ and MCBJ techniques can, however, be complicated by the fact that molecular junctions can break down before the molecules become fully extended.[3,24] In addition, the distance between electrodes may not match the extended molecular length as a result of varied molecular conformations and binding sites.[1,25] Molecular design offers a solution to minimize the effects resulting from conformational flexibility. In this vein, conjugated wires composed of aromatic building blocks, sometimes combined with alkynyl units, offer rigid wires with a length that is effectively independent of conformation. As an example, the length of oligo(aryleneethynylene)s (OAEs)[24] is independent of changes in conformation, although effective conjugation (and, thus, conductance) of OAEs varies as a function of rotation about single bonds that disrupts orbital overlap.[26,27]

Removing sp^2-carbon from the oligomeric framework of a wire leaves a molecule composed only of sp-hybridized carbon, namely polyynes. As linear, rigid, conjugated molecules, polyynes are viewed as attractive candidates for molecular wires, and, importantly, we expect that conjugation and electron transport along the sp-carbon chain should be effectively independent of rotation about the single bonds due to their cylindrical geometry in electronic structures.[1] Polyynes have been explored as molecular wires, both experimentally[28] and computationally.[29] Polyyne wires terminated with pyridyl groups can be effectively anchored to gold substrates,[9,30,31] and the series **Py[*n*]** with *n* = 1, 2, and 4 (Figure 1a) have been studied in STM-BJ experiments.[9,10] Derivatives longer than **Py[4]** (e.g., **Py[6]**) are, however, too unstable for analysis.[32] Rotaxination allows the examination of the hexayne **Py[6]•M** from the series of functionalized derivatives **Py*[*n*]** (Figure 1b).[30,33] Further exploration of pyridyl wires, however, requires an improved stabilization scheme to provide longer derivatives suitable for studies in devices. Recently reported polyynes **Py**[*n*]**[34] offer this opportunity (Figure 1c).

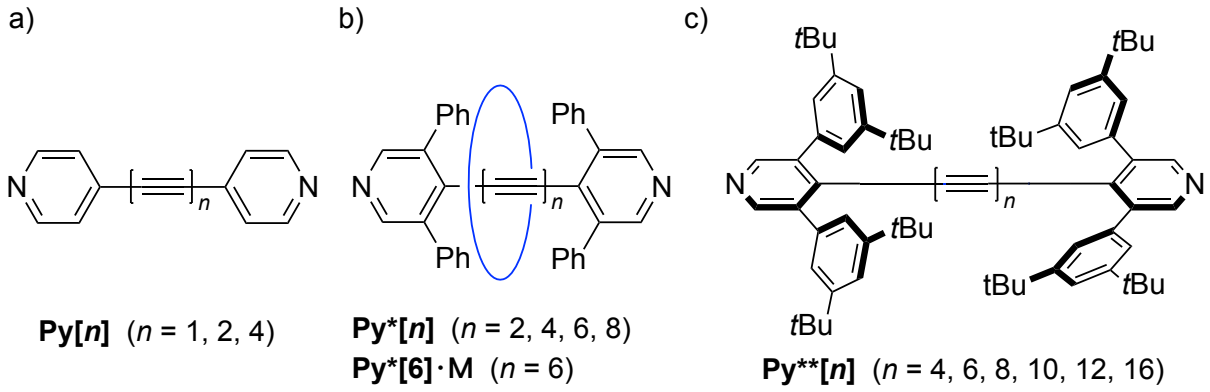

Figure 1. Polyynes endcapped with pyridyl groups as molecular wires: a) First generation wires **Py[*n*]** without functionalization, b) Stabilized polyynes **Py*[*n*]** through functionalization of the pyridyl groups (including the rotaxinated **Py*[6]·M** studied in ref. 30), and c) Stabilized wires **Py**[*n*]** through functionalization with di(*tert*-butylphenyl) groups.

In this report, we describe our investigations of the electrical conductance of the pyridyl endcapped polyynes **Py**[*n*]** (*n* = 4, 6, 8, 10, 12, 16), which includes a hexadecayne **Py**[16]**, consisting of 16 contiguous alkynes (32 *sp*-carbon atoms, Figure 1c). The synthesis of **Py**[*n*]** has been reported,[34] and the use of 3,5-bis(3,5-di-*tert*-butylphenyl)pyridyl group not only ensures the stability of long polyynes but also allows for effective bridging of the wires to gold electrodes. The relationship between molecular length and molecular properties, i.e., single-molecule conductance, has been established in this study through break-junction (BJ) experiments using a homemade scanning tunneling microscope (STM). We show a strong correlation between molecular lengths measured by molecular junction and those calculated by DFT methods (a range of 2–5 nm). This correspondence between experiment and theory is attributed to the rigid geometry of polyynes that fully extends across the electrode gap. Our measurements of single-molecule conductance demonstrate that charge transport in pyridyl polyynes occurs solely within the tunneling regime for distances of nearly 5 nm, exhibiting a single β value of 2.2 nm^{-1}. It is proposed that the conductance via tunneling is related to the effective conjugation length (ECL) of the series **Py**[*n*]**, as determined by UV-vis spectroscopic data analysis. These results define our understanding of the potential of polyynes as molecular wires.

Results and discussion

The operational principle of STM-BJ devices has been described elsewhere,[24] and a detailed description of the current measurements can be found in the SI. Briefly, samples are prepared from a dilute solution of each polyyne **Py**[n]** in CH_2Cl_2, with a typical concentration of ca. 1 mM, followed by deposition onto the gold surface via a dip-casting procedure under ambient conditions. During the STM-BJ experiment, the gold tip of the STM is driven in and out of contact with a gold substrate, while traces of conductance versus distance (*G* vs *z*) are collected. When a molecular junction forms while the electrodes are being separated, plateaus of conductance develop as the distance between the electrodes is increased until the molecular junction ultimately breaks. To determine the typical conductance and length of these molecular junctions, hundreds to thousands of traces of *G* vs *z* are recorded, followed by statistical analysis of those traces displaying conductance plateaus below $\log(G/G_0) = -1$, as determined via an automated process (see SI for details).

Molecular junctions formed with polyynes **Py**[n]** between gold electrodes have been analyzed and the results summarized in Figure 2a (see additional data in Figure S2 for individual traces *G* vs *z*). A distinct horizontal "cloud" is observed in the 2D conductance histograms. At $z < 0$, the short conductance cloud at $\log(G/G_0) \approx 0$ corresponds to a one-atom contact that forms before the final breakage of the gold contact. The $z = 0$ position corresponds to the breakage of gold tip-substrate contact. At $z > 0$, the conductance immediately decays to between $\log(G/G_0) = -4$ to -2, corresponding to the relaxation of the positions of the atoms at the apex of both the tip and substrate. This relaxation depends on the discrete arrangement of the apex atoms and opens an initial gap (the gold-retraction gap, L_{gap}) between the two electrodes of *ca.* 0.4 nm (Figure S3), which then increases as the retraction of the tip from the substrate continues.

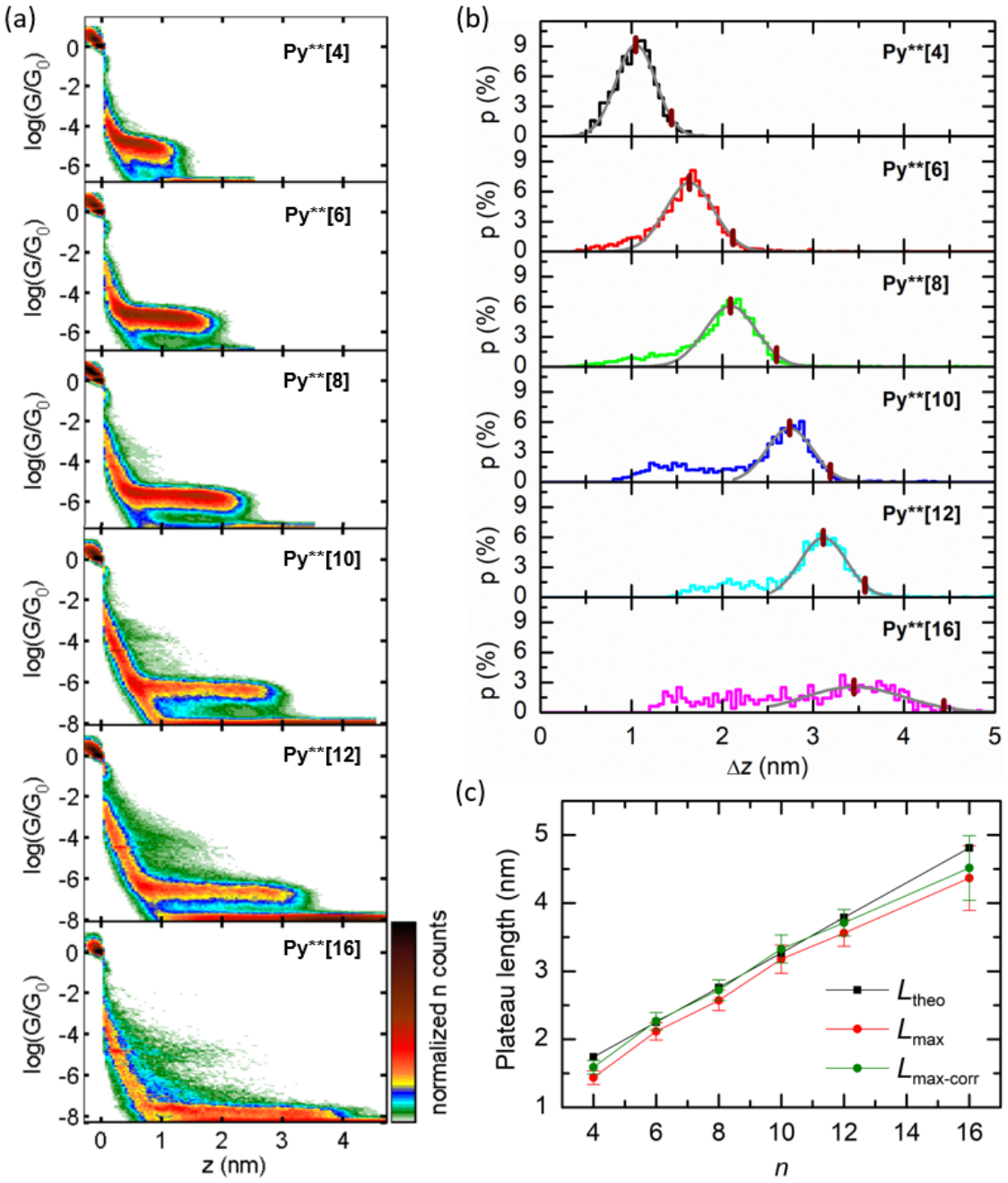

Figure 2. (a) 2D conductance histograms of compounds **Py**[*n*]** (*n* = 4, 6, 8, 10, 12, 16) as a function of distance *z*. The percentage of formed plateaus, as presented, over the overall recorded traces is as follows: 25% (**Py**[4]**), 43% (**Py**[6]**), 36% (**Py**[8]**), 24% (**Py**[10]**), 36% (**Py**[12]**), and 30% (**Py**[16]**). (b) Plateau-length distributions for compounds **Py**[*n*]** obtained from all traces with molecular plateaus. The mean length (L_{mean}) and the maximum length (L_{max}) for each distribution are indicated by short vertical purple lines. (c) Comparison of theoretical molecular lengths L_{theo} and experimental molecular lengths L_{max} and $L_{max\text{-}corr}$ as a function of polyyne length, *n*.

The extension of the main horizontal clouds depicted in Figure 2a provides information on the length for each compound in the molecular junction. Figure 2b shows the plateau-length distribution extracted from individual plateaus contributing to the main conductance cloud (see SI for details). In these distributions, as the polyyne length increases, the dominant peak progressively shifts to longer distances, *z*. Beginning with the hexayne **Py**[6]**, the dominant peak is accompanied by a secondary, less-intense peak at shorter distance. The secondary peak indicates the propensity of a fraction of molecular junctions to break down before full extension (see SI for details). Gaussian fits were performed for the prominent peak in each distribution, giving the most probable plateau length (peak maximum, L_{mean}) and the most extended plateau length (L_{max}) that is obtained as the length at which the Gaussian curve falls to a 20% of its maximum (both values indicated as short vertical purple ticks in Figure 2b). To compare these experimental values with the predicted molecular length L_{theo} (*N*-*N* distance), we used corrected lengths $L_{max\text{-}corr}$, obtained by subtracting the length of the *N*-Au bond ($L_{N\text{-}Au}$ = 0.25 nm)[25] from L_{max} and adding the gold-retraction gap (L_{gap} = 0.4 nm) described above (see SI for details). These data are summarized in Table 1, where L_{theo} is determined by density functional theory (DFT) at the B3LYP/6-311G* level.

Table 1. Summary of molecular length and single molecule conductance.

	Py[4]**	**Py**[6]**	**Py**[8]**	**Py**[10]**	**Py**[12]**	**Py**[16]**
$Log(G/G_0)$[a]	–5.0 ± 0.4	–5.2 ± 0.4	–5.7 ± 0.4	–6.3 ± 0.4	–6.6 ± 0.4	–7.8 ± 0.4
L_{theo} (nm)[b]	1.74	2.25	2.76	3.27	3.79	4.81
L_{mean} (nm)[a]	1.0 ± 0.2	1.6 ± 0.3	2.1 ± 0.3	2.7 ± 0.3	3.1 ± 0.3	3.4 ± 0.6
L_{max} (nm)[a]	1.4 ± 0.1	2.1 ± 0.1	2.6 ± 0.2	3.2 ± 0.2	3.6 ± 0.2	4.4 ± 0.5
$L_{max\text{-}corr}$ (nm)[c]	1.6 ± 0.1	2.3 ± 0.1	2.7 ± 0.2	3.3 ± 0.2	3.7 ± 0.2	4.5 ± 0.5

[a] The errors for $\log(G/G_0)$, L_{max}, and L_{mean}, are determined from the half width at half maxima of the gaussian fits. [b] L_{theo} determined by DFT calculations at the B3LYP/6-311G* level of theory. [c] $L_{max\text{-}corr} = L_{max} - L_{N\text{-}Au} + L_{gap} = L_{max} + 0.15$ nm.

The $L_{max\text{-}corr}$ values measured by STM-BJ range from 1.6 nm (**Py**[4]**) to 4.5 nm (**Py**[16]**) compare favorably with the theoretical plateau lengths L_{theo} (Figure 2c and Table 1) with a deviation of up to 0.3 nm in **Py**[16]**. The larger deviation for **Py**[16]** is likely influenced by the signal for this compound being close to the experimental noise floor, so that lowest conductance part of some of the plateaus is not accessible in the measurements. These STM-BJ experiments demonstrate that we are able to construct fully extended polyyne wires between gold electrodes and, thus, to obtain

the information on molecular length in addition to their corresponding conductance values.

Figure 3a shows the 1D conductance histograms for **Py**[4–16]**. It is worth noting that the histograms do not show the two-peak structure characteristically observed for 4,4'-bipyridine.[25,35] The two di(*tert*-butylphenyl) groups likely block any significant interaction between the electrodes and the face of the pyridyl ring. As such, binding takes place predominantly through the pyridine nitrogen (i.e., via a dative Au-*N* bond). The typical molecular conductance values, represented as $\log(G/G_0)$, are obtained from Gaussian fits to the conductance peaks in the histograms. Based on equation 1, there is a strong linear dependence of conductance on L_{theo}, expressed as $\log(G/G_0) = \log(G_c) - \beta L_{theo}\log(e)$, with an attenuation factor $\beta = 2.2 \pm 0.1$ nm^{-1} (Figure 3b). This experimental value of β for **Py**[*n*]** lies between the two previously reported values for oligoynes **Py[*n*]** with up to four triple bonds, namely $\beta = 0.6$ nm^{-1}[10] and $\beta = 3.1$ nm^{-1}.[9] The exponential decay of conductance with respect to molecular length suggests that electron transport is governed predominantly by a tunneling mechanism. Results from current *vs* voltage (*IV*) measurements show, in addition, that increasing the bias voltage from 0.1 V to 1.2 V produces a decrease in β of about 20% from $\beta = 2.2$ to 1.7 nm^{-1} (see SI). Increasing the bias voltage causes the chemical potential of the electrodes to approach the closest molecular resonance which, due to the decreasing HOMO−LUMO gap with length, becomes gradually closer as the length of the oligomer increases.[15] This behavior confirms that transport takes place within the HOMO−LUMO gap.

In the 2D histograms of Figure 2a, weaker clouds at higher conductance levels are observed, in addition to the main conductance clouds corresponding to the expected length of the fully-stretched junctions. We assign these weaker clouds to configurations of the junction in which the electrodes bind to the polyyne backbone and note that they account for only a small fraction of the traces displaying plateaus (<9% in all cases), likely due to the limited pi-surface featured by the polyyne wires. The data from the weaker clouds (at higher conductance) were not considered for the decay analysis in Figure 3b, as they would clearly affect the determination of β. Thus, only the data from the dominant junctions (at lower conductance) are considered in the analysis in Figure 3b (i.e., data from the length expected for complete end-to-end molecular extension between electrodes is achieved).

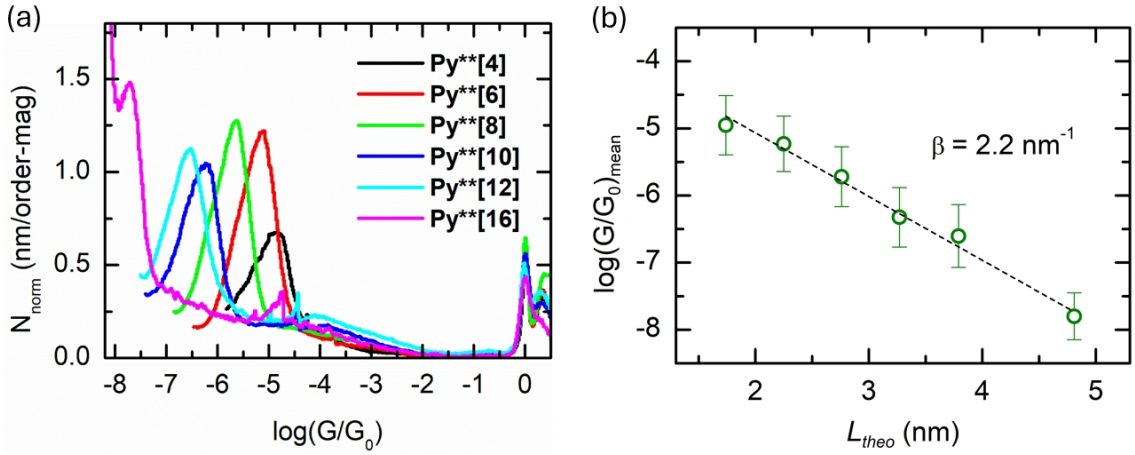

Figure 3. (a) Experimental 1D conductance histograms of compounds **Py**[*n*]**. (b) The semi-log plot of conductance log(G/G_0) versus the molecular length L_{theo} for **Py**[*n*]** based on the adaptation of eq 1 to give log(G/G_0) = log (G_c) – β L_{theo}log(e). The error bars correspond to the half width at the half maximum of the conductance peaks in Figure 3a.

Studies into the length-dependent conductance of carbon-based molecular wires in the past decades[1,36,37] have examined polyenes (sp^2-hybridized carbon)[6,38,39] and polyynes (sp-hybridized carbon)[1,9,10] as two typical models in one-dimensional systems. The extent of conjugation and, consequently, the length dependence conductance rely on the electronic coupling between neighboring sites. Tsuji and Hoffmann described a simple method based on a Hückel approach to predict β_N values for a polyene molecule (β_N is value per repeat unit of double and single bond).[40] The method determines the electronic coupling of the single and double bonds (t_S and t_D, respectively) using known bond lengths. The value β_N is expressed as the natural logarithm of the ratio of the electronic couplings, as shown in equation 2:

$$\beta_N = -2\ln\left(\frac{t_S}{t_D}\right) \qquad \text{(eq 2)}$$

$$\beta_N = -2\ln\left(\frac{t_S}{t_T}\right) \qquad \text{(eq 2')}$$

We have adapted this method here to predict β for polyynes using bond lengths compiled by Szafert and Gladysz from comprehensive analysis of published X-ray data of polyynes that gives mean single and triple bond lengths of 1.364 and 1.209 Å, respectively.[41] Equation 2 is now written in the form of eq 2', where t_T is the electronic coupling of a triple bond (full details are given in the Supporting Information). In doing so, we obtain β_N = 0.502 n^{-1} which then gives β = 1.95 nm^{-1}. The same analysis using

published X-ray data for **Py**[2]**, **Py**[4]**, **Py**[6]**, and **Py**[8]**,[34] gives single and triple bond lengths of 1.357 Å and 1.207 Å, respectively, and β = 1.90 nm^{-1} (full details are given in SI). Considering the simplicity of the model, this value agrees very well with the experimental β value of 2.2 nm^{-1}. It is intriguing to compare the resulting polyynes with the polyenes. Tsuji and Hoffmann calculated β_N values of 0.28 to 0.37 n^{-1} for polyenes using eq 2,[40] which is lower than that for a polyyne. The lower values for polyenes is consistent with the fact that the value of t_S/t_D is closer to 1 than t_S/t_T. These calculated values of β_N for polyenes are, however, notably lower than the reported experimental values, which are in the range β_N = 0.4–0.6 n^{-1}, giving β = 1.6–2.4 nm^{-1} (i.e., similar to polyynes).[40] This discrepancy is indicative of distortions in the structures of polyenes under experimental conditions as a result of rotation about single bonds, which ultimately diminish the electronic coupling. These conformational affects are not accounted for in the simple model described above using eq 2 and are absent in polyynes due to their cylindrical electron distribution (and, thus, electronic coupling independent of bond rotations). The good agreement between the predicted and measured values of β for polyynes, therefore, suggests that the conductance is unaffected by bond rotations.

A remarkable aspect of the conductance of **Py**[*n*]** is the absence of a transition from tunneling to hopping regimes in the series **Py**[*n*]**, even at the longest molecular length of **Py**[16]** (*ca*. 5 nm). We posit that the dominance of the tunneling mechanism results from the significant effective conjugation length (ECL) of **Py**[*n*]** series, which is predicted to be n > 30, as determined through experimental UV-vis and Raman data.[34] Similar predictions for ECL have been made for other series of polyynes.[34,42-45] For comparison, oligo(aryleneethynylene)s (OAEs), which also have a rigid and linear structure, present the transition from tunneling to hopping in the range of 2.5–3 nm (ca. n = 4–5) via either STM-BJ[24,46,47] or conducting probe atomic force microscopy (CP-AFM).[24,46,47] This is consistent with the ECL of n = 5 as determined by Meier et al. on the basis of UV-vis spectroscopic data analysis.[27] The dampened ECL for OAEs results from variations of dihedral angles between aryl rings, resulting in reduced p-orbital overlap (reduced conjugation); contributions from the aromaticity of the aryl rings also likely contributes.[48] For a series of oligo(phenyleneimine)s, on the other hand, the transition from tunneling to hopping occurs at ca. 4 nm (n = 5–6) based on measurements by CP-AFM,[49, 50] concurrent with a longer ECL (n = 5–7) and

consistent with better delocalization through the imine than the alkyne. Similarly, Frisbie and coworkers reported the related imine-based structure oligo(naphthalene-fluoreneimine)s (ONIs) wires in which the transition to hopping occurred at ca. 4–5 nm (n = 4–5) via CP-AFM analysis[51] with an ECL of n = 5–6 (see SI for details). Finally, the partial planarization of polyphenylenes through the incorporation of fluorene segments increases conjugation and results a transition to hopping between 5.2–7.3 nm in STM-BJ devices.[52] These findings are nicely consistent with the posited relationship between the ECL and the experimentally observed transition from tunneling to hopping mechanisms. The series of polyynes **Py**[*n*]** features ECL > 8 nm (at n = 30), which is consistent with the tunneling dominance observed here through the longest studied derivative **Py**[*n*]** with a length of ca. 5 nm.

Conclusions

We have examined the conductance of a series of polyynes endcapped with pyridyl groups and featuring unprecedented molecular lengths, e.g., **Py**[*n*]** (n = 4, 6, 8, 10, 12, 16). The polyynic wires feature well-defined lengths up to *ca.* 5 nm, and molecular junctions with these wires have been constructed and characterized by scanning tunneling microscopy break junctions (STM-BJ). Excellent agreement between the length of the molecular junction and the calculated molecular length of the polyynes is established, and the observed conductance decay is predominantly due to off-resonant tunneling with an attenuation value β of 2.2 nm^{-1}. The series of six polyynic wires studied, featuring lengths up to four times greater than in previous studies of polyynes, determines the β value to an unprecedented level of confidence.

The experimental determination of molecular length and conductance of polyyne wires **Py**[*n*]** provides convincing details into the relationship between molecular structure and properties. We have applied a simple model to interpret the experimental β value, as well as other conjugated carbon chains, which suggests that electronic coupling (and thus, conductance) in the single and triple bonds of polyynes is unaffected by the rotation about the single bonds. We propose the tunneling regime continues, without a transition to hopping, due to the long ECL of polyynes, which is estimated to be $n \geq 30$ (L > 8 nm).

ASSOCIATED CONTENT

Supplemental Information includes a description of molecular structure, details of STM-BJ experiments and length analyses, and determination of ECL for oligonaphthalene-fluoreneimines.

.

AUTHOR INFORMATION

Yueze Gao – orcid.org/0000-0002-1856-7959
Edmund Leary – orcid.org/0000-0001-7541-5997
M. Teresa González – orcid.org/0000-0002-7253-797X
Matthew Johnson – orcid.org/0000-0001-5134-0986
Rik R. Tykwinski –orcid.org/0000-0002-7645-4784

AUTHOR CONTRIBUTIONS

R.R.T., M.K., and M.T.G. designed the project. Y.G. designed, synthesized, and characterized all compounds. E.L., M.T.G., and L.P.R. performed conductivity measurements and analysis. M.J. performed theoretical calculations. All authors discussed the results, as well as contributed to writing and editing the manuscript.

ACKNOWLEDGMENT

The authors in Canada are grateful for financial support from the Natural Sciences and Engineering Research Council of Canada (NSERC) and Canada Foundation for Innovation (CFI), and authors in Spain acknowledge support from Spanish MICIN (MCIN/AEI/10.13039/501100011033) through BIINTEL (PID2021-127964NB-C21), CNS2023-145464, DECOSMOL (EIGConcertJapan, PCI2023-143389), the Comunidad de Madrid Atracción de Talento grant 2019-T1/IND-16384 and the 'Severo Ochoa' Programme for Centres of Excellence in R&D (CEX2020-001039-S). Initial synthetic work at FAU was supported by the German Research Council (DFG), SFB 953 “Synthetic Carbon Allotropes”. Y.G. acknowledges funding from China Scholarship Council (CSC).

References

(1) Bryce, M. R. A Review of Functional Linear Carbon Chains (Oligoynes, Polyynes, Cumulenes) and Their Applications as Molecular Wires in Molecular Electronics and Optoelectronics. *J. Mater. Chem. C* **2021**, *9*, 10524–10546.

(2) Perrin, M. L.; Burzurí, E.; van der Zant, H. S. J. Single-Molecule Transistors. *Chem. Soc. Rev.* **2015**, *44*, 902–919.

(3) Evers, F.; Korytar, R.; Tewari, S.; van Ruitenbeek, J. M. Advances and Challenges in Single-Molecule Electron Transport. *Rev. Mod. Phys.* **2020**, *92*, 035001.

(4) Li, X. L.; He, J.; Hihath, J.; Xu, B. Q.; Lindsay, S. M.; Tao, N. J. Conductance of Single Alkanedithiols: Conduction Mechanism and Effect of Molecule-Electrode Contacts. *J. Am. Chem. Soc.* **2006**, *128*, 2135–2141.

(5) Li, C.; Pobelov, I.; Wandlowski, T.; Bagrets, A.; Arnold, A.; Evers, F. Charge Transport in Single Au | Alkanedithiol | Au Junctions: Coordination Geometries and Conformational Degrees of Freedom. *J. Am. Chem. Soc.* **2008**, *130*, 318–326.

(6) He, J.; Chen, F.; Li, J.; Sankey, O. F.; Terazono, Y.; Herrero, C.; Gust, D.; Moore, T. A.; Moore, A. L.; Lindsay, S. M. Electronic Decay Constant of Carotenoid Polyenes from Single-Molecule Measurements. *J. Am. Chem. Soc.* **2005**, *127*, 1384–1385.

(7) Meisner, J. S.; Kamenetska, M.; Krikorian, M.; Steigerwald, M. L.; Venkataraman, L.; Nuckolls, C. A Single-Molecule Potentiometer. *Nano Lett.* **2011**, *11*, 1575–1579.

(8) Published reports for polyynes rely on a somewhat restricted set of molecules with a maximum of four triple bonds, and some studies limited to only 2–3 compounds, potentially limiting the accuracy in determining β.

(9) Moreno-Garcia, P.; Gulcur, M.; Manrique, D. Z.; Pope, T.; Hong, W. J.; Kaliginedi, V.; Huang, C. C.; Batsanov, A. S.; Bryce, M. R.; Lambert, C.; et al. Single-Molecule Conductance of Functionalized Oligoynes: Length Dependence and Junction Evolution. *J. Am. Chem. Soc.* **2013**, *135*, 12228–12240.

(10) Wang, C.; Batsanov, A. S.; Bryce, M. R.; Martín, S.; Nichols, R. J.; Higgins, S. J.; García-Suárez, V. M.; Lambert, C. J. Oligoyne Single Molecule Wires. *J. Am. Chem. Soc.* **2009**, *131*, 15647–15654.

(11) Zang, Y. P.; Fu, T. R.; Zou, Q.; Ng, F.; Li, H. X.; Steigerwald, M. L.; Nuckolls, C.; Venkataraman, L. Cumulene Wires Display Increasing Conductance with Increasing Length. *Nano Lett.* **2020**, *20*, 8415–8419.

(12) Xu, W. J.; Leary, E.; Hou, S.; Sangtarash, S.; Gonzalez, M. T.; Rubio-Bollinger, G.; Wu, Q. Q.; Sadeghi, H.; Tejerina, L.; Christensen, K. E.; et al. Unusual Length Dependence of the Conductance in Cumulene Molecular Wires. *Angew. Chem. Int. Ed.* **2019**, *58*, 8378–8382.

(13) Xu, W. J.; Leary, E.; Sangtarash, S.; Jirasek, M.; Gonzalez, M. T.; Christensen, K. E.; Vicente, L. A.; Agrait, N.; Higgins, S. J.; Nichols, R. J.; et al. A Peierls Transition in Long

Polymethine Molecular Wires: Evolution of Molecular Geometry and Single-Molecule Conductance. *J. Am. Chem. Soc.* **2021**, *143*, 20472–20481.
(14) Gunasekaran, S.; Hernangomez-Perez, D.; Davydenko, I.; Marder, S.; Evers, F.; Venkataraman, L. Near Length-Independent Conductance in Polymethine Molecular Wires. *Nano Lett.* **2018**, *18*, 6387–6391.
(15) Leary, E.; Limburg, B.; Alanazy, A.; Sangtarash, S.; Grace, I.; Swada, K.; Esdaile, L. J.; Noori, M.; Gonzalez, M. T.; Rubio-Bollinger, G.; et al. Bias-Driven Conductance Increase with Length in Porphyrin Tapes. *J. Am. Chem. Soc.* **2018**, *140*, 12877–12883.
(16) Martin, R. E.; Pannier, M.; Diederich, F.; Gramlich, V.; Hubrich, M.; Spiess, H. W. Determination of End-to-End Distances in a Series of TEMPO Diradicals of up to 2.8 nm Length with a New Four-Pulse Double Electron Electron Resonance Experiment. *Angew. Chem. Int. Ed.* **1998**, *37*, 2834–2837.
(17) Siera, H.; Mehrparvar, S.; Fax, J.; Kreuzahler, M.; Haberhauer, G. Measurement of Nanometer Distances in Solution via (13) C NMR Spectroscopy-Shrinking of Macrocycles with Increasing Temperature. *Angew. Chem. Int. Ed.* **2023**, *62*, e202301465.
(18) Gao, Y.; Walter, V.; Ferguson, M. J.; Tykwinski, R. R. Hierarchical Synthesis, Structure, and Photophysical Properties of Gallium- and Ruthenium-Porphyrins with Axially Bonded Azo Ligands. *Chem. Eur. J.* **2020**, *26*, 16712–16720.
(19) Mathew-Fenn, R. S.; Das, R.; Silverman, J. A.; Walker, P. A.; Harbury, P. A. A Molecular Ruler for Measuring Quantitative Distance Distributions. *Plos One* **2008**, *3*, e3229.
(20) Kalinin, S.; Peulen, T.; Sindbert, S.; Rothwell, P. J.; Berger, S.; Restle, T.; Goody, R. S.; Gohlke, H.; Seidel, C. A. M. A Toolkit and Benchmark Study for FRET-Restrained High-Precision Structural Modeling. *Nat. Methods* **2012**, *9*, 1218–1225.
(21) Zang, Y. P.; Zou, Q.; Fu, T. R.; Ng, F.; Fowler, B.; Yang, J. J.; Li, H. X.; Steigerwald, M. L.; Nuckolls, C.; Venkataraman, L. Directing Isomerization Reactions of Cumulenes with Electric Fields. *Nat. Commun.* **2019**, *10*, 4482.
(22) Lin, J.; Lv, Y.; Song, K.; Song, X.; Zang, H.; Du, P.; Zang, Y.; Zhu, D. Cleavage of Non-polar C(sp2)–C(sp2) Bonds in Cycloparaphenylenes via Electric Field-Catalyzed Electrophilic Aromatic Substitution. *Nat. Commun.* **2023**, *14*, 293.
(23) Leary, E.; Roche, C.; Jiang, H.-W.; Grace, I.; González, M. T.; Rubio-Bollinger, G.; Romero-Muñiz, C.; Xiong, Y.; Al-Galiby, Q.; Noori, M.; et al. Detecting Mechanochemical Atropisomerization within an STM Break Junction. *J. Am. Chem. Soc.* **2018**, *140*, 710–718.
(24) Zhao, X.; Huang, C.; Gulcur, M.; Batsanov, A. S.; Baghernejad, M.; Hong, W.; Bryce, M. R.; Wandlowski, T. Oligo(aryleneethynylene)s with Terminal Pyridyl Groups: Synthesis and Length Dependence of the Tunneling-to-Hopping Transition of Single-Molecule Conductances. *Chem. Mater.* **2013**, *25*, 4340–4347.

(25) Kamenetska, M.; Quek, S. Y.; Whalley, A. C.; Steigerwald, M. L.; Choi, H. J.; Louie, S. G.; Nuckolls, C.; Hybertsen, M. S.; Neaton, J. B.; Venkataraman, L. Conductance and Geometry of Pyridine-Linked Single-Molecule Junctions. *J. Am. Chem. Soc.* **2010**, *132*, 6817–6821.
(26) Siemsen, P.; Livingston, R. C.; Diederich, F. Acetylenic Coupling: A Powerful Tool in Molecular Construction. *Angew. Chem. Int. Ed.* **2000**, *39*, 2632–2657.
(27) Meier, H.; Stalmach, U.; Kolshorn, H. Effective conjugation length and UV/vis spectra of oligomers. *Acta Polym.* **1997**, *48*, 379–384.
(28) Zieleniewska, A.; Zhao, X. T.; Bauroth, S.; Wang, C. S.; Batsanov, A. S.; Calderon, C. K.; Kahnt, A.; Clark, T.; Bryce, M. R.; Guldi, D. M. Resonance-Enhanced Charge Delocalization in Carbazole-Oligoyne-Oxadiazole Conjugates. *J. Am. Chem. Soc.* **2020**, *142*, 18769–18781.
(29) Garner, M. H.; Bro-Jorgensen, W.; Solomon, G. C. Three Distinct Torsion Profiles of Electronic Transmission through Linear Carbon Wires. *J. Phys. Chem. C* **2020**, *124*, 18968–18982.
(30) Milan, D. C.; Krempe, M.; Ismael, A. K.; Movsisyan, L. D.; Franz, M.; Grace, I.; Brooke, R. J.; Schwarzacher, W.; Higgins, S. J.; Anderson, H. L.; et al. The Single-Molecule Electrical Conductance of A Rotaxane-Hexayne Supramolecular Assembly. *Nanoscale* **2017**, *9*, 355–361.
(31) Gulcur, M.; Moreno-García, P.; Zhao, X.; Baghernejad, M.; Batsanov, A. S.; Hong, W.; Bryce, M. R.; Wandlowski, T. The Synthesis of Functionalised Diaryltetraynes and Their Transport Properties in Single-Molecule Junctions. *Chem. Eur. J.* **2014**, *20*, 4653–4660.
(32) Wang, C.; Jia, H.; Li, H.; Wang, Y. 1,12-bis (4-pyridyl) -1,3,5,7,9,11-dodecyl-hexayne: synthesis and properties. *Jilin Huagong Xueyuan Xuebao* **2012**, *20*, 33–36.
(33) Krempe, M.; Lippert, R.; Hampel, F.; Ivanovic-Burmazovic, I.; Jux, N.; Tykwinski, R. R. Pyridyl-Endcapped Polyynes: Stabilized Wire-like Molecules. *Angew. Chem. Int. Ed.* **2016**, *55*, 14802–14806.
(34) Gao, Y.; Hou, Y.; Gordillo Gámez, F.; Ferguson, M. J.; Casado, J.; Tykwinski, R. R. The loss of endgroup effects in long pyridyl-endcapped oligoynes on the way to carbyne. *Nat. Chem.* **2020**, *12*, 1143–1149.
(35) Aradhya, S. V.; Frei, M.; Hybertsen, M. S.; Venkataraman, L. Van der Waals interactions at metal/organic interfaces at the single-molecule level. *Nat. Mater.* **2012**, *11*, 872-876.
(36) Xin, N.; Guan, J.; Zhou, C.; Chen, X.; Gu, C.; Li, Y.; Ratner, M. A.; Nitzan, A.; Stoddart, J. F.; Guo, X. Concepts in the Design and Engineering of Single-Molecule Electronic Devices. *Nat. Rev. Phys.* **2019**, *1*, 211–230.

(37) Su, T. A.; Neupane, M.; Steigerwald, M. L.; Venkataraman, L.; Nuckolls, C. Chemical Principles of Single-Molecule Electronics. *Nat. Rev. Mater.* **2016**, *1*, 16002.
(38) Dell, E. J.; Capozzi, B.; Xia, J.; Venkataraman, L.; Campos, L. M. Molecular Length Dictates the Nature of Charge Carriers in Single-Molecule Junctions of Oxidized Oligothiophenes. *Nat. Chem.* **2015**, *7*, 209–214.
(39) Visoly-Fisher, I.; Daie, K.; Terazono, Y.; Herrero, C.; Fungo, F.; Otero, L.; Durantini, E.; Silber, J. J.; Sereno, L.; Gust, D. Conductance of a Biomolecular Wire. *Proc. Natl. Acad. Sci.* **2006**, *103*, 8686–8690.
(40) Tsuji, Y.; Movassagh, R.; Datta, S.; Hoffmann, R. Exponential Attenuation of Through-Bond Transmission in a Polyene: Theory and Potential Realizations. *ACS Nano* **2015**, *9*, 11109–11120.
(41) Szafert, S.; Gladysz, J. A. Carbon in One Dimension: Structural Analysis of the Higher Conjugated Polyynes. *Chem. Rev.* **2006**, *106*, Pr1–Pr33.
(42) Gao, Y.; Tykwinski, R. R. Advances in Polyynes to Model Carbyne. *Acc. Chem. Res.* **2022**, *55*, 3616–3630.
(43) Chalifoux, W. A.; Tykwinski, R. R. carbon allotrope carbyne. *Nat. Chem.* **2010**, *2*, 967–971.
(44) Arora, A.; Baksi, S. D.; Weisbach, N.; Amini, H.; Bhuvanesh, N.; Gladysz, J. A. Monodisperse Molecular Models for the sp Carbon Allotrope Carbyne; Syntheses, Structures, and Properties of Diplatinum Polyynediyl Complexes with PtC(20)Pt to PtC(52)Pt Linkages. *ACS Cent. Sci.* **2023**, *9*, 2225–2240.
(45) Patrick, C. W.; Gao, Y.; Gupta, P.; Thompson, A. L.; Parker, A. W.; Anderson, H. L. Masked alkynes for synthesis of threaded carbon chains. *Nat. Chem.* **2024**, *16*, 193–200.
(46) Lu, Q.; Yao, C.; Wang, X. H.; Wang, F. S. Enhancing Molecular Conductance of Oligo(p-phenylene ethynylene)s by Incorporating Ferrocene into Their Backbones. *J. Phys. Chem. C* **2012**, *116*, 17853–17861.
(47) Lu, Q.; Liu, K.; Zhang, H. M.; Du, Z. B.; Wang, X. H.; Wang, F. S. From Tunneling to Hopping: A Comprehensive Investigation of Charge Transport Mechanism in Molecular Junctions Based on Oligo(p-phenylene ethynylene)s. *Acs Nano* **2009**, *3*, 3861–3868.
(48) Martin, R. E.; Diederich, F. Linear Monodisperse π-Conjugated Oligomers: Model Compounds for Polymers and More. *Angew. Chem. Int. Ed.* **1999**, *38*, 1350–1377.
(49) Nguyen, Q. V.; Frisbie, C. D. Hopping Conductance in Molecular Wires Exhibits a Large Heavy-Atom Kinetic Isotope Effect. *J. Am. Chem. Soc.* **2021**, *143*, 2638–2643.
(50) Choi, S. H.; Kim, B.; Frisbie, C. D. Electrical Resistance of Long Conjugated Molecular Wires. *Science* **2008**, *320*, 1482–1486.

(51) Choi, S. H.; Risko, C.; Delgado, M. C. R.; Kim, B.; Bredas, J. L.; Frisbie, C. D. Transition from Tunneling to Hopping Transport in Long, Conjugated Oligo-imine Wires Connected to Metals. *J. Am. Chem. Soc.* **2010**, *132*, 4358–4368.
(52) Hines, T.; Diez-Perez, I.; Hihath, J.; Liu, H. M.; Wang, Z. S.; Zhao, J. W.; Zhou, G.; Muellen, K.; Tao, N. J. Transition from Tunneling to Hopping in Single Molecular Junctions by Measuring Length and Temperature Dependence. *J. Am. Chem. Soc.* **2010**, *132*, 11658–11664.

TOC Graphic: